E-ISSN: 2321–9637
Volume 1, Issue 5, December 2013
International Journal of Research in Advent Technology
Available Online at: http://www.ijrat.org

INFLUENCE OF DOPING OF RARE EARTH ION(RE=La) ON STRUCTURAL, ELECTRICAL AND DIELECTRIC PROPERTIES OF SrM-HEXAFERRITE

Arun Katoch [a] , Taminder Singh [b] , B.S Sandhu[c]
[a] *Department of Physics, Research Scholar, India.*
Email : arunkatoch24@gmail.com
[b] *Department of Physics , Khalsa College, Amritsar, Punjab, India*
[c] *Department of Applied Sciences BKSJ Engineering College , Amritsar , India.*

Abstract :
A series of M- type hexagonal ferrite samples $Sr_{1-x}La_xFe_{12}O_{19}$ (x = 0.0, 0.10, 0.20 and 0.30) were prepared by employing the ceramic technique. The samples were characterized by X-ray diffraction and scanning electron microscope.AC conductivity and dielectric properties have been studied for a series of M-type hexagonal spinal ferrite with composition $Sr_{1-x}La_xFe_{12}O_{19}$ as a function of frequency and temperature. The result of AC conductivity was discussed in terms of quantum mechanical tunneling and small polaron tunneling models. The dielectric constant (ε') , Dielectric loss tangent (tanδ) and AC conductivity (σ_{AC}) as a function of frequency from 20 Hz to 1 MHz were found to increase with increasing temperature due to the increase of the hopping frequency, while they decrease with increasing La ion content due to reduction of iron ions available for the conduction process.

Keywords: Hexagonal ferrites, XRD, SEM, AC conductivity , Dielectric Constant (ε'),Dielectric loss (tanδ)

1. INTRODUCTION

M-type hexagonal ferrites, with nominal chemical formula $MFe_{12}O_{19}$ (M= Ba ,Sr)represent for many years now the largest volume fraction of the permanent magnet market , mainly due to their low cost ,which is compensating for their moderate magnetic performance.. These materials are in the category of magnetic semiconductors. Their electrical and dielectric properties depends on the preparation conditions , such as sintering temperature , sintering atmosphere and soaking time as well as the type of substituted ions. It was proposed that the air sintered ferrites are characterized by microstructure consisting of relatively high conductive grains separated by high grain boundaries [1,2] . The common processing method of hexagonal ferrites are conventional ceramic process of solid –state reaction [3], co-precipitation /hydro-thermal synthesis[4,5], sol-gel process[6], spray pyrolysis[7] and molten salt method[8,9]. The conventional ceramic process, which include mixing the raw materials, calcinations, milling, pressing and sintering at 1200 – 1350^0 C , has been often used in industrial manufacturing.

This work aims at synthesizing La substituted SrM hexaferrite by conventional ceramic technique and study the influence of doping of rare earth ion La on the structural , electrical and dielectric behavior of $Sr_{1-x}La_xFe_{12}O_{19}$ hexaferrite. The AC conductivity and dielectric properties have been studied for a series of M-type hexagonal spinal ferrite with composition $Sr_{1-x}La_xFe_{12}O_{19}$ as a function of frequency and temperature.

2. EXPERIMENTAL DETAILS

2.1. Synthesis

A series of $Sr_{1-x}La_xFe_{12}O_{19}$ samples with different substitution ratios were prepared by a standard ceramic processing technique [10-13]. High purity materials $SrCO_3$, La_2O_3 and Fe_2O_3 procured from LOBA CHEMIE

E-ISSN: 2321–9637
Volume 1, Issue 5, December 2013
International Journal of Research in Advent Technology
Available Online at: http://www.ijrat.org

PVT. LTD. Mumbai (India) were used as starting raw materials and were mixed together in the appropriate composition, calculated from the following chemical reaction

$$(1-x)\ SrCO3 + 6\ Fe_2O_3 + (x/2)\ La_2O_3 \rightarrow Sr_{1-x}La_xFe_{12}O_{19} + (1-x)CO_2 + (x/4)O_2 \quad (1)$$

Where, x varies from 0.0 to 0.3 with an increment of 0.1 . The powders so obtained were mixed in distilled water and milled for 6 hours in an agate motor and pestle fitted with an electric grinder rotating at a speed of 100 RPM. After grinding the powders were dried in hot air. The powders thus dried were calcined at 1200^0C for six hours in a resistance furnace at a controlled heating and cooling rate (5^0C/min.). The calcined powders were further wet- milled in distilled water for 8 hours to obtain very fine and uniform size powders. After milling the powders were again dried and 5% polyvinyl alcohol was added to it , which acts as binder. These materials were then granulated through sieves of 60-80 mesh B.S.S (250-180 µm approximately). The granules were cold pressed in a die at a compressed pressure of 75 KN to produce pellets of 14.5 mm diameter and 3.0 mm to 4.0 mm thickness. These pellets were finally sintered at 1250^0C for 2 hours. The samples were cooled in the furnace itself to room temperature Katoch et al.[14]

2.2. Measurement details

In order to analyze the phase structure of prepared samples, X- Ray diffraction(XRD) (XPERT-PRO) analysis was performed with CuK_α (λ = 1.5406) radiations. The crystal structure of the samples was examined by using a X-ray diffractometer. The microstructure was investigated using scanning electron microscope (SEM, JEOL-JSM 6100). Using sputtering technique, specimens were coated by an Au thin film before observations in SEM. The DC electrical conductivity (σ) of all the samples was measured at room temperature by two probe method . The specimen was connected through a dry battery of 1.5 to 3 V Keithley electrometer (Model 6517A), for measuring the current. AC conductivity and dielectric measurements of all ferrites samples were measured (HP4284A) with standard two-probe technique [15].

The AC conductivity was calculated by using the formula

$$\sigma_{AC} = \frac{Gt}{A} \quad (2)$$

Where t and A are thickness and cross-sectional area of pellets and G is the conductance. The value of dielectric constant (ε') of the ferrite samples can be calculated by using the following formula

$$\varepsilon' = \frac{C_p t}{\varepsilon_o A} \quad (3)$$

Where C_p is the capacitance of samples in pf, t the thickness of the samples in cm, A the cross-sectional area of the samples in sq.cm and ε_0 the permittivity in free space having value 8.854×10^{-2} pf/cm. Katoch et al. [14]

3. RESULT AND DISCUSSION

3.1. Influence of doping on structural behavior

Fig.1 shows the typical XRD pattern of $Sr_{1-x}La_xFe_{12}O_{19}$ ferrite for different molar concentration in the prepared samples sintered at 1250^oC for 6h which shows almost single magnetoplumbite structure and analysis reveals that the prepared samples were almost single hexagonal M-type Phase. In the doped ferrite cases, the dopants La seem to dissolve /arrange in the hexagonal structure to fulfill the formation of single hexagonal phase. In case of La^{3+} substitution, the samples are single hexagonal M-type phase. No peaks of

E-ISSN: 2321–9637
Volume 1, Issue 5, December 2013
International Journal of Research in Advent Technology
Available Online at: http://www.ijrat.org

Fe_2O_3 and La_2O_3 phases are observed, which suggest that Sr^{2+} ion is substituted by La^{3+}ions.

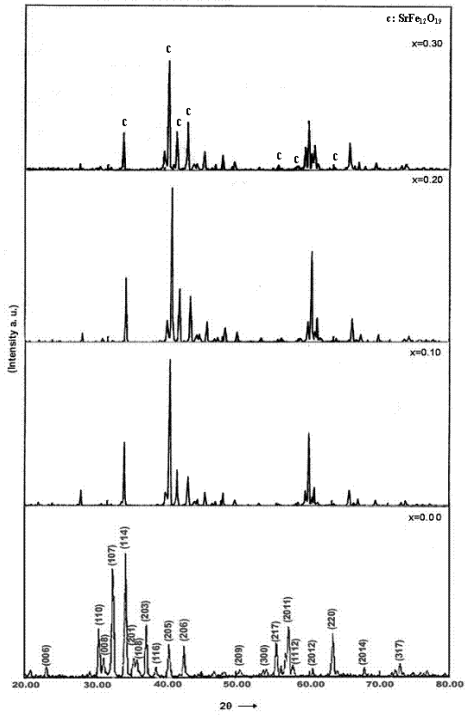

Fig.1 X-ray patterns of La substituted samples after calcinations for $Sr_{1-x}La_xFe_{12}O_{19}$ series (X=0.0, 0.10, 0.20 and 0.30)

3.2 Influence of doping on microstructure

Microstructure plays a key role in obtaining the desired electric, dielectric and magnetic properties for these materials. Figs. 1(a-d) show the SEM images of the fractured surface of all the samples. Fig.1. (a) is for the undoped sample whereas Fig. 1. (b-d) is for La doped samples. The important feature in all the microstructures is the existence of hexagonal faceted grains which are randomly oriented. Using SEM micrographs, the average grain size of all the doped and undoped samples was calculated. It is observed that the average grain size decreased for all substituted samples relative to undoped sample[16]. The doping inhibits the grain growth phenomenon [17]. This leads to the observed decrease of the grain size and hence responsible for the enhancement of coercivity.

E-ISSN: 2321–9637
Volume 1, Issue 5, December 2013
International Journal of Research in Advent Technology
Available Online at: http://www.ijrat.org

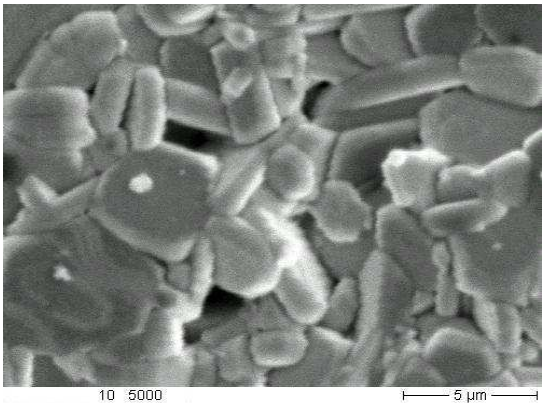

La (X=0.0) (a)

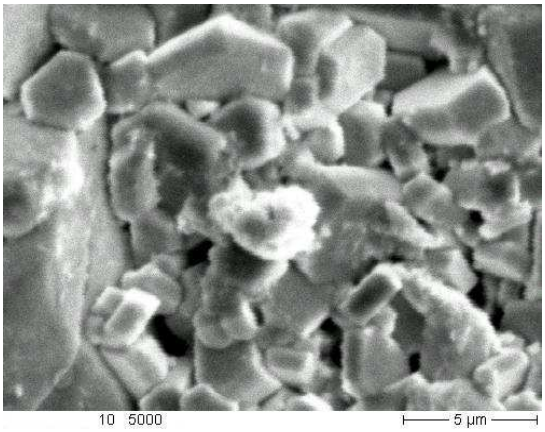

La (X=0.10) (b)

La (X=0.20) (c)

E-ISSN: 2321–9637
Volume 1, Issue 5, December 2013
International Journal of Research in Advent Technology
Available Online at: http://www.ijrat.org

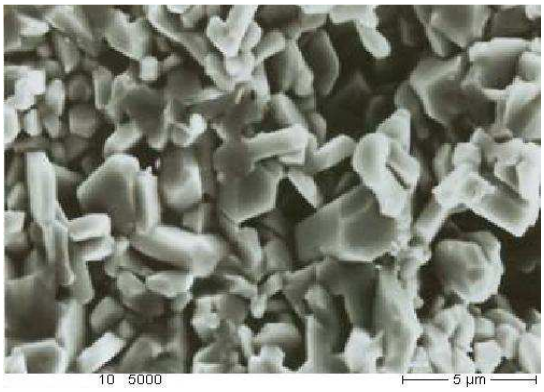

La (X=0.30) (d)

Fig. 1(a-d) SEM images for the $Sr_{1-x}RE_xFe_{12}O_{19}$ where RE = La^{3+}(x = 0 to 0.30).

3.3. Variation of AC Conductivity with Frequency

The results of the real AC conductivity σ_{AC} as a function of frequency at different temperatures for three series prepared with RE = La^{3+}, are shown in the Figs. 2(a-d)respectively. It is shown that AC conductivity σ_{AC} is independent at lower frequencies but above a certain frequency, it becomes dependent i.e. its value increases with an increase in frequency. The increase in σ_{AC} is more rapid at lower temperature and slower at higher temperature for all samples. At high temperatures, the AC conductivity becomes almost frequency independent. Similar type of trend has been reported for Cu-Cr ferrites [18] and Ni-Mg ferrites [19]. The conduction mechanism in ferrite is explained on the basis of hopping of charge carrier between Fe^{2+} and Fe^{3+} ions on octahedral site. The increase in frequency enhances the hopping frequency of charge carriers resulting in an increase in the conduction process thereby increasing the conductivity. Ferrites are low mobility materials and increase in conductivity does not mean that the number of charge carrier increases, but only the mobility of charge carriers increases. Furthermore, at high temperatures, the conductivity becomes almost independent to frequency, because the hopping frequency no more follows the external field and thus lags behind it. Also increase in AC conductivity with the increase of RE^{3+} ions is observed. The results of AC conductivity can be explained on the basis of the assumption that real AC conductivity consists of two parts [20]

$$\sigma' = \sigma_{DC} + \sigma_{AC} \quad (2)$$

The first term σ_{DC} is the DC conductivity, which is frequency independent and can be written as

$$\sigma_{DC} = \sigma_0 \exp(-E/KT) \quad (3)$$

where E is the activation energy for electronic conduction, σ_0 is a pre-exponential constant and k is the Boltzmann's constant. The second term σ_{AC} is the temperature as well as frequency dependent and is given by [20, 21].

$$\sigma_{AC} = B(T)\,\omega^{n}(T) \quad (4)$$

where B is the parameter having units of conductivity (Ω^{-1} cm^{-1}) , n is dimensionless exponent and is temperature and compositional dependent where $\omega = 2\pi f$, is the angular frequency.

E-ISSN: 2321–9637
Volume 1, Issue 5, December 2013
International Journal of Research in Advent Technology
Available Online at: http://www.ijrat.org

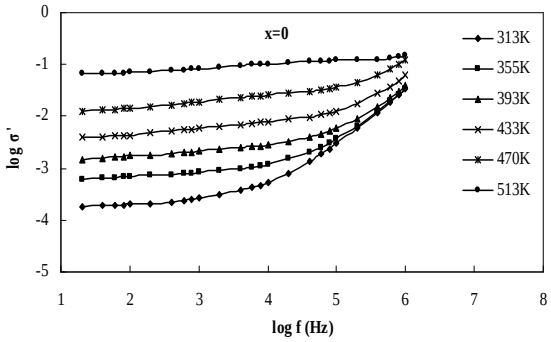

(a)

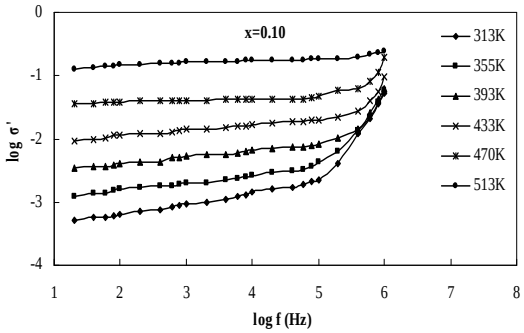

(b)

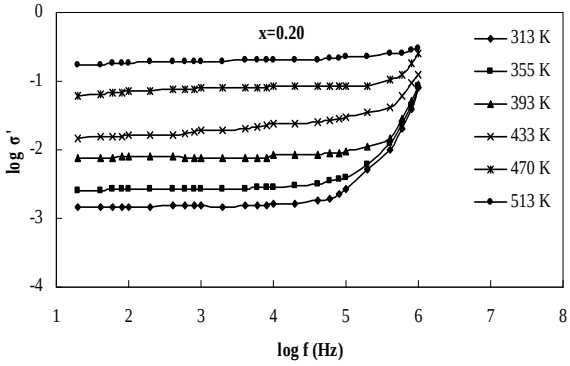

(c)

E-ISSN: 2321–9637
Volume 1, Issue 5, December 2013
International Journal of Research in Advent Technology
Available Online at: http://www.ijrat.org

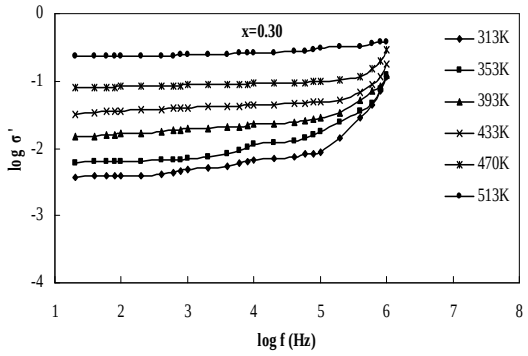

(d)

Fig.2(a-d) Frequency dependence of AC conductivity of $Sr_{1-x}La_xFe_{12}O_{19}$ at different temperatures with compositions (X= 0.0 , 0.10, 0.20 and 0.30)

3.4. Variation of AC Conductivity with Temperature

The temperature variation of real part of AC conductivity at the selected frequencies (1 KHz, 10 KHz, 100 KHz, 600 KHz and 1 MHz) for three series prepared with RE = La^3 are shown in the Figs. 3(a-d) respectively.

The results of plot of log σ_{AC} against $10^3/T$ show that σ_{AC} exhibits a semi- conductive behaviour with the temperature, where the AC conductivity increases with increasing temperature. The results of AC conductivity could be explained on the basis of Koops Model [1], which assumes that ferrite samples act as a multilayer capacitor in which the ferrite grain and grain boundaries have different properties. According to this model, the bulk material of the ferrite could be considered as consisting two layers, one represents the grains (a conducting layer) and the other represents the grain boundaries (a poor conducting layer). The grain have high conductivity are effective at high frequencies. However the grain boundaries have low conductivity and are effective at lower frequencies.

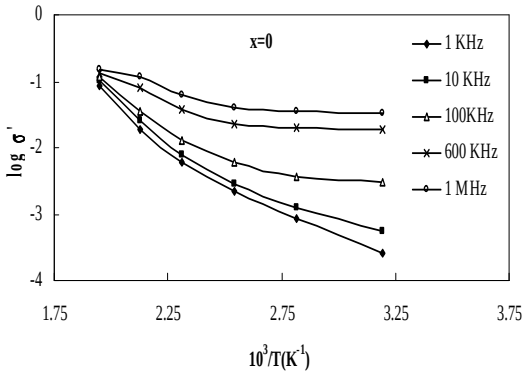

(a)

E-ISSN: 2321–9637
Volume 1, Issue 5, December 2013
International Journal of Research in Advent Technology
Available Online at: http://www.ijrat.org

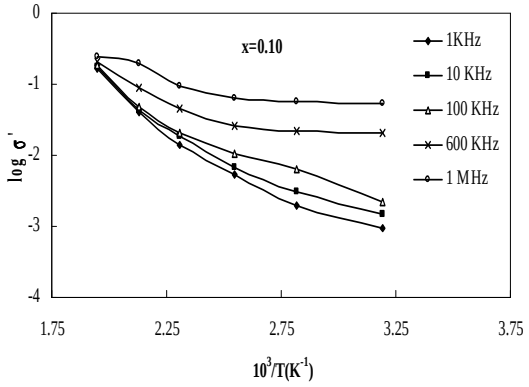

(b)

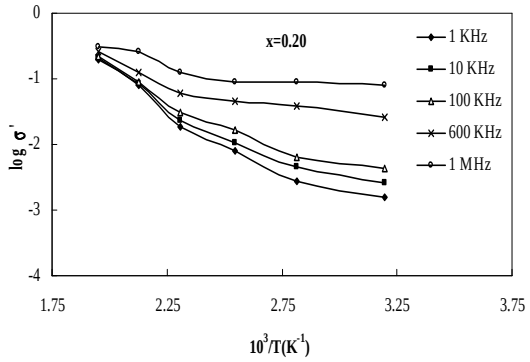

(c)

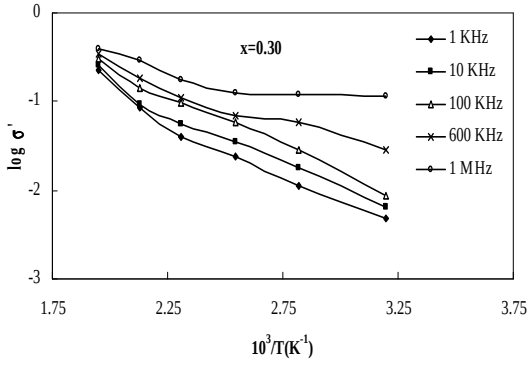

(d)

Fig.3(a-d) Temperature dependence of AC conductivity of $Sr_{1-x}La_xFe_{12}O_{19}$ at different frequencies with compositions(X= 0.0 , 0.10 , 0.20 and 0.30)

3.5. Dielectric Constant Variation with Frequency

The variation of the dielectric constant as a function of frequency at a constant temperature of 304 K for three series prepared with RE = La^{3+} are shown in Figs. 4(a – d) respectively. It is observed that the value of dielectric constant decreases with increasing frequency. This behaviour in rare earth substituted Sr hexaferrite is common

E-ISSN: 2321–9637
Volume 1, Issue 5, December 2013
International Journal of Research in Advent Technology
Available Online at: http://www.ijrat.org

ferromagnetic behaviour and has also been observed by other investigators [22-24]. A more dielectric dispersion is observed at lower frequency range and it remains almost independent of applied external field at high frequency domain. The dielectric dispersion observed at lower frequency range is due to Maxwell -Wagner type interfacial polarization well in agreement with the Koop's phenomenological theory [1],[25]. According to these models, the dielectric material with a heterogeneous structure can be imagined as a structure consists of well conducting grains separated by highly resistive thin layers (grain boundaries). In this case, the applied voltage on the sample drops mainly across the grain boundaries and space charge polarization is built up at the grain boundaries.

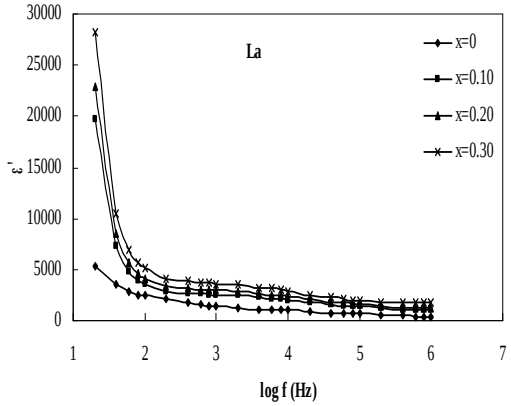

Fig.4.Variation of dielectric constant (ε′) with frequency for $Sr_{1-x}La_xFe_{12}O_{19}$ series.

3.5. Dielectric Loss Tangent Variation with Frequency

The variation of the dielectric loss tangent as a function of frequency at a constant temperature of 304 K for three series prepared with RE = La^{3+} is shown in Figs. 4. respectively. This figure explicitly show that the value of dielectric loss tangent increases as the frequency increases to attain its maximum (peak) value at a certain critical frequency followed by decrease at higher frequencies. The peaking behaviour in the dielectric loss occurs when the jump frequency of electron between Fe^{2+} and Fe^{3+} is equal to the frequency of the applied field [26, 27].

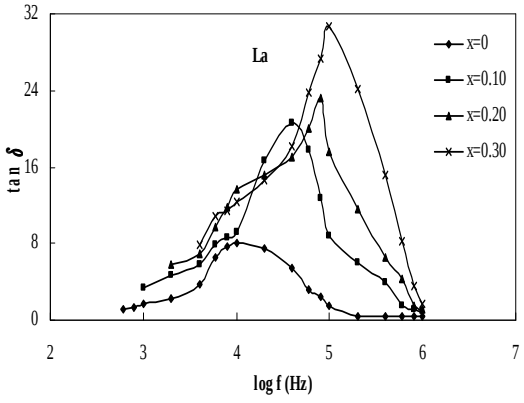

Fig.5. Variation of dielectric loss (tan δ) with frequency for $Sr_{1-x}La_xFe_{12}O_{19}$ series(X= 0.0 , 0.10, 0.20 and 0.30)

E-ISSN: 2321–9637
Volume 1, Issue 5, December 2013
International Journal of Research in Advent Technology
Available Online at: http://www.ijrat.org

4. CONCLUSION

The average grain size decreased for all substituted samples. It was found that the average grain size estimated from SEM was approximately 5µm and it was almost dependent on the composition (X= 0.0, 0.10, 0.20 and 0.30).The electrical properties of SrM samples depend on the synthesis parameters(milling power and milling time). For low milling power, high densities samples do not have the highest dielectric constant . The polarization generated from the grain boundary contributes to a higher dielectric constant for intermediate milling time samples. In addition , it could be shown that increasing milling time the resonance frequency decreases .The value of dielectric constant (ε'), dielectric loss tangent ($\tan\delta$) and AC conductivity of $Sr_{1-x}La_xFe_{12}O_{19}$ are strongly dependent on the frequency , applied voltage and dose rate, which further increases after irradiation. Also, value of ε' and ε'' increases with increasing dose rate , but decrease with increasing frequencies . The AC conductivity σ_{AC} increases with increasing dose rate and frequency .

REFERENTES

[1]. Koops, C.G .,phys.Rev.83(1951)121
[2]. A. Dias, R.Luiz Moreire, J. Mater. Res. 12 (8) (1998) 2190 Koops, C.G .,phys.Rev.83(1951)121
[3]. A. Dias, R.Luiz Moreire, J. Mater. Res. 12 (8) (1998) 2190
[4]. F.Harberey, A. Kockel, IEEE Trans. Magn. 12 (1976) 983
[5]. J.H. Lee, H.H. Lee, C.W. Won, J.Kor. Inst.Met. Mater. 33(1995)21
[6] K..Haneda ,C. Miyakawa,H. Kojima, J. Amer. Ceram. Soc. 57(1974) 354
[7] H.Zhang , L.Li, J.Zhou, Yue, Z. Ma, Z. Gui, J .Eur. ceram. Soc. 21(2001)149
[8] Y. Hayashi, T.Kanazawa, T. yamaguchi,, J.mater.Sci.21(1986)2876
[9]. T. Kimura, T. Takahashi, Yamaguchi, J.Mater. Sci. 15(1980)1491
[10]. Herring, C., J. Appl. Phys., **21 (5),** 437 (1950).
[11]. Kuczynski, G.C., J. Appl. Phys., **21,** 632 , (1950)
[12]. Coble, R.L., J. Appl. Phys., **32,** 793 (1961).
[13]. Coble, R.L. and Burke, J.E., "Progress in Ceramic Science", (The Macmillon Co., New York, 1963)
[14]. Katoch, Arun , Singh, Anterpreet. IJERSTE , Vol. 2 issue 2, Feb.-2013
[15]. Fang, T.T and Lee, K.T., J. Am. Ceram. Soc., **72**, 2304 (1989).
[16]. Sharma, P., Verma, A., Sidhu, R.K and Pandey, O.P., Magn. Magn. Mater. **307,** 157 (2006).
[17]. Sattar, A.A., Wafik, A.H., El- Shokrofy, K.M and Tabby, M.M.El., Phys. Stat.Sol. (a)., **171,** 563 (1999).
[18]. Ahmed, M., El Hiti, M., Mosaad, M an Attia, S., J. Magn. Magn. Mater.,**146,** 84 (1995).
[19]. El Hiti, M.A., J. Phys. D: Appl. Phys., **29,** 501 (1996).
[20] Jonscher, A.K., "Dielectric Relaxation in Solids",(Chelsea Dielectric Press,London, 1983).
[21] Mostafa, M.F., Kader, M.M. Abd. El., Atallah, A.S and Nimr, M.K. El., Phys. Stat. Sol. (a)., **135,** 549 (1993).
[22]. Ravinder, D., Vijaya, P and Reddy, B., Mater. Lett., **57,** 4344 (2003).
[23]. Shaikh, A.M., Belled, S.S and Chougule, B.K., J. Magn. Magn. Mater., **195,** 384 (1999).
[24]. Kumar, B.R and Ravinder, D., Mater. Lett., **53,** 437 (2002).
[25]. Wagner, K.W., Ann. Phys., **40,** 817 (1973)..
[26]. Reddy, M.B and Reddy, P.V., J. Appl. Phys., **24,** 975 (1991).
[27]. Abo El Ata, A.M., Attia, S.M and Meaz, T.M., Solid Stat. Sci., **6,** 61 (2004).